Modeling of Melt Layer Erosion and Splashing during Plasma Instabilities

Gennady V. Miloshevsky

Ahmed Hassanein

Purdue University, West Lafayette, Indiana

Presented at the 15th International Workshop on Spherical Tori 2009, U. Wisconsin, Madison, WI, U.S.A., October 22-24, 2009

Outline

- Classical Analysis of Kelvin-Helmholtz Instability
- Modelling of Kelvin-Helmholtz Instability

Kelvin-Helmholtz Instability

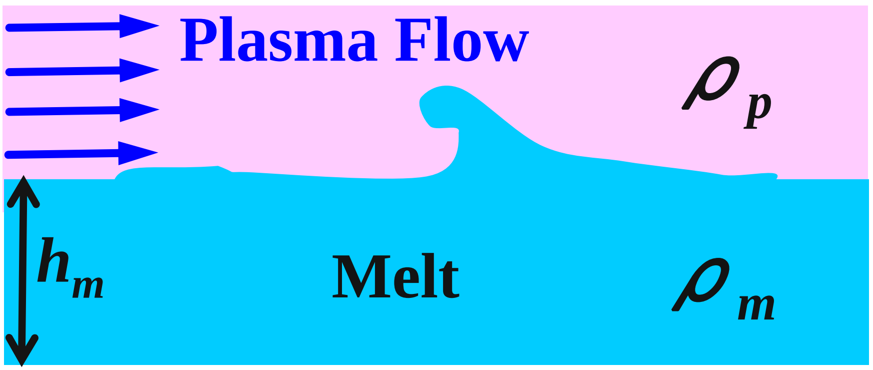

Question: can the K-H instability develop under these plasma flow conditions with finger-like projections that break off to form droplets?

$V_p \sim 10^6$ cm/s

$\rho_p \sim 10^{-9}$ g/cm^3

$V_m \sim 0 \div 10^3$ cm/s

If the K-H instability can develop, then

- what is a minimal wavelength and the speed of plasma flow?
- what is the effect of the depth of melt layer?
- what is the effect of a magnetic field and its direction with respect to plasma flow?

for Li : ***$\rho_m \sim 0.512$ g/cm^3 $\quad h_m \sim 0.2$ cm***

for W : ***$\rho_m \sim 17.6$ g/cm^3 $\quad h_m \sim 0.04$ cm***

Classical K-H Instability Analysis

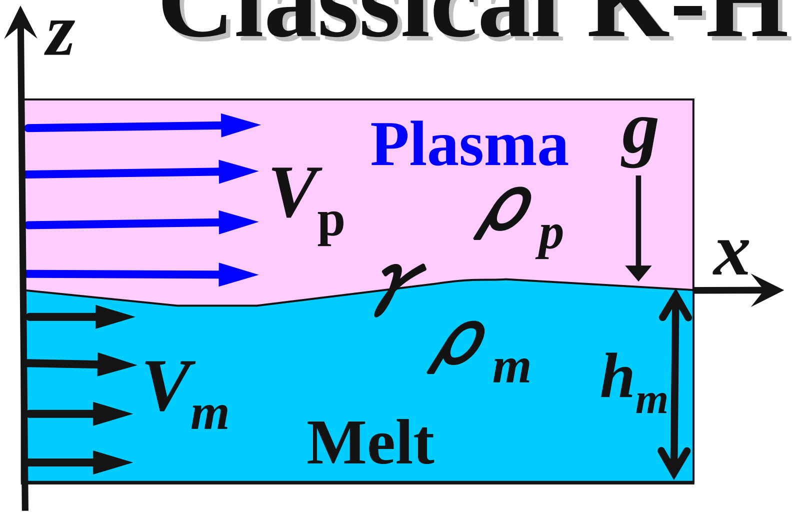

Sketch of the parallel flow of plasma and melt streaming respectively with velocity V_p and V_m, of densities ρ_p and ρ_m ($\rho_m >> \rho_p$) and of interfacial tension γ. Gravity acts in the negative z-direction.

$V_p \sim 10^6$ cm/s

$\rho_p \sim 10^{-9}$ g/cm^3

$g \sim 981$ cm/s^2

for W : ***$\gamma \sim 2300$ dyn/cm***

$\rho_m \sim 17.6$ g/cm^3

for Li : ***$\gamma \sim 405$ dyn/cm***

$\rho_m \sim 0.512$ g/cm^3

Surface perturbation of the form:

$$z = z_0 e^{i(k_x x + k_y y + nt)}$$

The curvature of the surface:

$$K = \kappa^2 z_0 e^{i(k_x x + k_y y + nt)}$$

$$\text{with} \quad \kappa = \sqrt{k_x^2 + k_y^2}$$

The pressure at the interface:

$$p_p = p_m + \gamma K$$

Classical K-H Instability Analysis

Classical dispersion relation:

$$n = -k_x\left(\frac{\rho_m V_m + \rho_p V_p}{\rho_m + \rho_p}\right) \pm \left[\left(g\kappa\frac{\rho_m - \rho_p}{\rho_m + \rho_p} + \frac{\kappa^3\gamma}{\rho_m + \rho_p}\right) tanh(\kappa h_m) - \frac{k_x^2\rho_m\rho_p}{(\rho_m + \rho_p)^2}(V_m - V_p)^2\right]^{1/2}$$

phase velocity of waves

stabilizing gravity for long waves

stabilizing tension for short waves

destabilizing inertia

Instability $\longrightarrow$ $\frac{\kappa^2\rho_m\rho_p}{(\rho_m + \rho_p)^2}(V_m - V_p)^2 > \left(g\kappa\frac{\rho_m - \rho_p}{\rho_m + \rho_p} + \frac{\kappa^3\gamma}{\rho_m + \rho_p}\right) tanh(\kappa h_m)$

Minimize this inequality relative κ to find a cut-off wavenumber from the condition: $\frac{\partial f(\kappa)}{\partial \kappa}_{|\kappa=\kappa_c} = 0 \quad \Rightarrow$

$$\kappa_c h_m (F + \gamma\kappa_c^2)(tanh^2(\kappa_c h_m) - 1) + (F - \gamma\kappa_c^2) tanh(\kappa_c h_m) = 0$$

$F = g(\rho_m - \rho_p)$ - gravitational restoring force

Non-linear Equation

Chandrasekhar, S. 1961, Hydrodynamic and Hydromagnetic Stability, Oxford University Press, Oxford.

Classical K-H Instability Analysis

The case of deep melt: $h_m \to \infty \quad \Rightarrow \quad tanh(\kappa_c h_m) \to 1$

$$F - \gamma\kappa_c^2 = 0 \quad \Rightarrow \kappa_c = \sqrt{\frac{g(\rho_m - \rho_p)}{\gamma}}$$

Cut-off wavelength

$$\lambda_c = 2\pi\sqrt{\frac{\gamma}{g(\rho_m - \rho_p)}}$$

Criterion for the velocity difference

$$\left(V_m - V_p\right)^2 > \frac{4\pi\gamma}{\lambda_c}\frac{\left(\rho_m + \rho_p\right)}{\rho_m\rho_p}$$

The case of finite-depth melt:

numerical solution of the **Non-linear Equation** is required to find a cut-off wavenumber and wavelength and to determine the minimal relative speed for generation of the K-H instability

Chandrasekhar, S. 1961, Hydrodynamic and Hydromagnetic Stability, Oxford University Press, Oxford.

Classical K-H Instability Analysis

Magnetic field in the direction of flow

$$n = -k_x\left(\frac{\rho_m V_m + \rho_p V_p}{\rho_m + \rho_p}\right) \pm \left[\left(g\kappa\frac{\rho_m - \rho_p}{\rho_m + \rho_p} + \frac{\kappa^3(\gamma + \gamma_H)}{\rho_m + \rho_p}\right)tanh(\kappa h_m) - \frac{k_x^2 \rho_m \rho_p}{(\rho_m + \rho_p)^2}(V_m - V_p)^2\right]^{1/2}$$

phase velocity of the waves

stabilizing gravity for long waves

stabilizing tension for short waves

destabilizing inertia

$$\gamma_H = \frac{\mu H^2}{2\pi}\frac{k_x^2}{\kappa^3}$$ - magnetic surface tension

$$|V_m - V_p| \leq \sqrt{\frac{\mu H^2}{2\pi}\frac{(\rho_m + \rho_p)}{\rho_m \rho_p}}$$

- the K-H instability will be additionally suppressed by a magnetic field if the relative speed does not exceed the root-mean-square Alfven speed

Magnetic field transverse to the direction of flow

the dispersion relation is not changed

- development of the K-H instability in the direction of the flow is unaffected by a magnetic field transverse to this flow direction

Chandrasekhar, S. 1961, Hydrodynamic and Hydromagnetic Stability, Oxford University Press, Oxford.

Classical K-H Instability Analysis

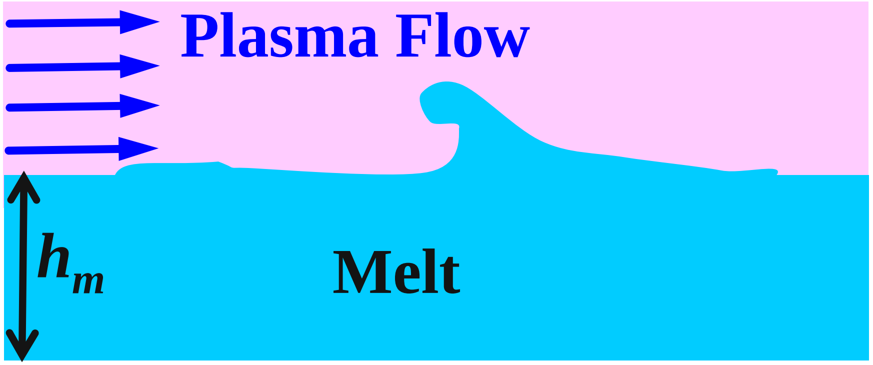

The case of a melt layer with infinite depth $h_m \rightarrow \infty$

$V_p \sim 10^6$ cm/s

$\rho_p \sim 10^{-9}$ g/cm^3

for Li :

$\lambda_c \sim 5.64$ cm

$V_c \sim 9.5 \cdot 10^5$ cm/s

for W :

$\lambda_c \sim 2.29$ cm

$V_c \sim 3.6 \cdot 10^6$ cm/s

- perturbations with wavelengths smaller than a cut-off ~5.64 cm for Li and ~2.29 cm for W will be stable due to suppression by surface tension
- waves can be created on the surface with a wavelength greater than a cut-off when the relative velocity exceeds ~$9.5 \cdot 10^5$ cm/s for Li and ~$3.6 \cdot 10^6$ cm/s for W

PURDUE
UNIVERSITY

Classical K-H Instability Analysis

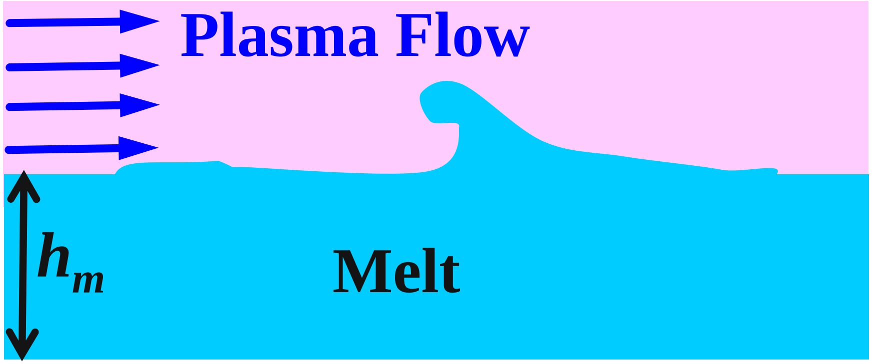

The case of a melt layer with finite depth h_m – Non-linear Equation is solved numerically to find a cut-off λ_c for each h_m

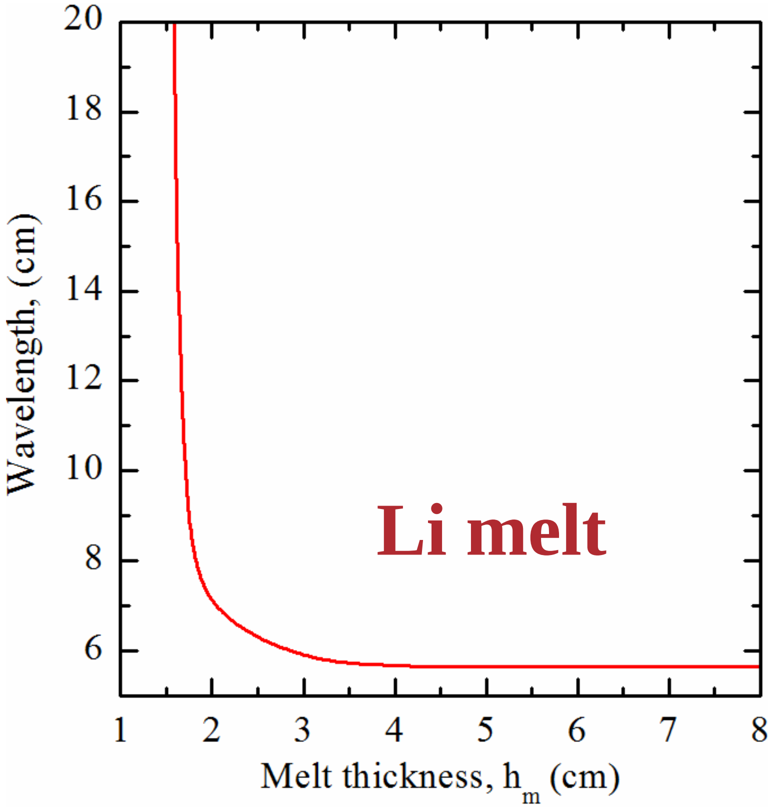

- cut-off wavelength *increases* with decrease of the thickness of a melt layer; it diverges for small melt depth ~1.5 cm
- relative velocity *decreases* with decrease of the thickness h_m of a melt layer

Classical K-H Instability Analysis Summary

- waves with wavelengths below cut-offs, ~5.6 cm for Li and ~2.3 cm for W, will be *suppressed* on the surface of a deep melt due to tension effects

- cut-off wavelength *increases* with decrease of the thickness of a melt layer

- magnetic field *transverse* to the direction of the melt flow has no the effect on development of the K-H instability

Two-Fluid Computational Model

- fluids with different physical and thermodynamic properties (out of thermodynamic equilibrium)
- fluids are separated by sharp interface and co-exist at every point in space and time with certain volume fractions

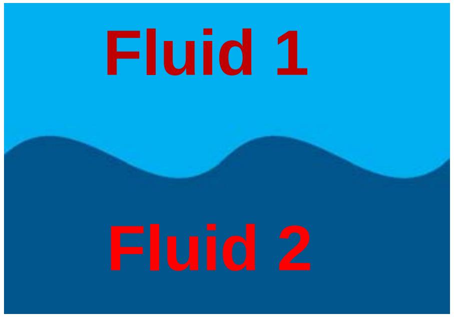

- each fluid is governed by its own set of balance equations closed by its own equation of state
- pressure and velocity relaxation procedures are used to establish the mechanical equilibrium between fluids
- source terms can be included for dissipative processes and phase transitions; equations for the number density of bubbles, granules, etc. can be added

Two-Fluid Computational Model

Mass conservation: ***plasma and liquid phase***

$$\frac{\partial \alpha_g \rho_g}{\partial t} + \frac{\partial \alpha_g \rho_g u_g}{\partial x} + \frac{\partial \alpha_g \rho_g v_g}{\partial y} + \frac{\partial \alpha_g \rho_g w_g}{\partial z} = 0$$

$$\frac{\partial \alpha_l \rho_l}{\partial t} + \frac{\partial \alpha_l \rho_l u_l}{\partial x} + \frac{\partial \alpha_l \rho_l v_l}{\partial y} + \frac{\partial \alpha_l \rho_l w_l}{\partial z} = 0$$

α_g and α_l - gas and liquid volume fractions

$$\alpha_g + \alpha_l = 1$$

Two-Fluid Computational Model

Momentum conservation: ***plasma phase***

$$\frac{\partial \alpha_g \rho_g u_g}{\partial t} + \frac{\partial}{\partial x}\left(\alpha_g \rho_g u_g^2 + \alpha_g p_g\right) + \frac{\partial}{\partial y}\left(\alpha_g \rho_g u_g v_g\right) + \frac{\partial}{\partial z}\left(\alpha_g \rho_g u_g w_g\right) = \\ = P_I \frac{\partial \alpha_g}{\partial x} + \lambda\left(u_l - u_g\right) - \alpha_g \rho_g g$$

$$\frac{\partial \alpha_g \rho_g v_g}{\partial t} + \frac{\partial}{\partial x}\left(\alpha_g \rho_g v_g u_g\right) + \frac{\partial}{\partial y}\left(\alpha_g \rho_g v_g^2 + \alpha_g p_g\right) + \frac{\partial}{\partial z}\left(\alpha_g \rho_g v_g w_g\right) = \\ = P_I \frac{\partial \alpha_g}{\partial y} + \lambda\left(v_l - v_g\right)$$

$$\frac{\partial \alpha_g \rho_g w_g}{\partial t} + \frac{\partial}{\partial x}\left(\alpha_g \rho_g w_g u_g\right) + \frac{\partial}{\partial y}\left(\alpha_g \rho_g w_g v_g\right) + \frac{\partial}{\partial y}\left(\alpha_g \rho_g w_g^2 + \alpha_g p_g\right) = \\ = P_I \frac{\partial \alpha_g}{\partial z} + \lambda\left(w_l - w_g\right)$$

Two-Fluid Computational Model

Momentum conservation: ***liquid phase***

$$\frac{\partial \alpha_l \rho_l u_l}{\partial t} + \frac{\partial}{\partial x}\left(\alpha_l \rho_l u_l^2 + \alpha_l p_l\right) + \frac{\partial}{\partial y}\left(\alpha_l \rho_l u_l v_l\right) + \frac{\partial}{\partial z}\left(\alpha_l \rho_l u_l w_l\right) =$$

$$= -P_I \frac{\partial \alpha_g}{\partial x} - \lambda(u_l - u_g) - \alpha_l \rho_l g$$

$$\frac{\partial \alpha_l \rho_l v_l}{\partial t} + \frac{\partial}{\partial x}\left(\alpha_l \rho_l v_l u_l\right) + \frac{\partial}{\partial y}\left(\alpha_l \rho_l v_l^2 + \alpha_l p_l\right) + \frac{\partial}{\partial z}\left(\alpha_l \rho_l v_l w_l\right) =$$

$$= -P_I \frac{\partial \alpha_g}{\partial y} - \lambda(v_l - v_g)$$

$$\frac{\partial \alpha_l \rho_l w_l}{\partial t} + \frac{\partial}{\partial x}\left(\alpha_l \rho_l w_l u_l\right) + \frac{\partial}{\partial y}\left(\alpha_l \rho_l w_l v_l\right) + \frac{\partial}{\partial y}\left(\alpha_l \rho_l w_l^2 + \alpha_l p_l\right) =$$

$$= -P_I \frac{\partial \alpha_g}{\partial z} - \lambda(w_l - w_g)$$

Two-Fluid Computational Model

Energy conservation: ***plasma and liquid phase***

$$\frac{\partial \alpha_g E_g}{\partial t} + \frac{\partial}{\partial x}\left(u_g(\alpha_g E_g + \alpha_g p_g)\right) + \frac{\partial}{\partial y}\left(v_g(\alpha_g E_g + \alpha_g p_g)\right) + \frac{\partial}{\partial z}\left(w_g(\alpha_g E_g + \alpha_g p_g)\right) =$$

$$= U_I P_I \frac{\partial \alpha_g}{\partial x} + V_I P_I \frac{\partial \alpha_g}{\partial y} + W_I P_I \frac{\partial \alpha_g}{\partial z} + \mu P_I (p_l + \sigma\kappa - p_g) +$$

$$+ \lambda U_I (u_l - u_g) + \lambda V_I (v_l - v_g) + \lambda W_I (w_l - w_g) - \alpha_g \rho_g u_g g$$

$$\frac{\partial \alpha_l E_l}{\partial t} + \frac{\partial}{\partial x}\left(u_l(\alpha_l E_l + \alpha_l p_l)\right) + \frac{\partial}{\partial y}\left(v_l(\alpha_l E_l + \alpha_l p_l)\right) + \frac{\partial}{\partial z}\left(w_l(\alpha_l E_l + \alpha_l p_l)\right) =$$

$$= -U_I P_I \frac{\partial \alpha_g}{\partial x} - V_I P_I \frac{\partial \alpha_g}{\partial y} - W_I P_I \frac{\partial \alpha_g}{\partial z} - \mu P_I (p_l + \sigma\kappa - p_g) -$$

$$- \lambda U_I (u_l - u_g) - \lambda V_I (v_l - v_g) - \lambda W_I (w_l - w_g) - \alpha_l \rho_l u_l g$$

σ – surface tension coefficient; for tungsten σ =2300 dyn/cm

$\kappa = -\nabla \cdot \left(\frac{\nabla \alpha_l}{|\nabla \alpha_l|} \right)$ - interface curvature

Two-Fluid Computational Model

Volume fraction equation

$$\frac{\partial \alpha_g}{\partial t} + U_I \frac{\partial \alpha_g}{\partial x} + V_I \frac{\partial \alpha_g}{\partial y} + W_I \frac{\partial \alpha_g}{\partial z} = -\mu(p_l + \sigma\kappa - p_g)$$

Stiffened equations of state

$$\rho_g e_g = (p_g + \gamma_g P_{\infty,g})/(\gamma_g - 1); \quad \rho_l e_l = (p_l + \gamma_l P_{\infty,l})/(\gamma_l - 1).$$

$$E_g = \frac{1}{2}\rho_g(u_g^2 + v_g^2 + w_g^2) + \rho_g e_g; \quad E_l = \frac{1}{2}\rho_l(u_l^2 + v_l^2 + w_l^2) + \rho_l e_l.$$

Interface pressure and velocities

for tungsten:

$\gamma_l = 2.2$

$P_{\infty,l} = 1.41\ Mbar$

$$P_I = \alpha_g p_g + \alpha_l p_l; \quad U_I = \frac{\alpha_g \rho_g u_g + \alpha_l \rho_l u_l}{\alpha_g \rho_g + \alpha_l \rho_l};$$

$$V_I = \frac{\alpha_g \rho_g v_g + \alpha_l \rho_l v_l}{\alpha_g \rho_g + \alpha_l \rho_l}; \quad W_I = \frac{\alpha_g \rho_g w_g + \alpha_l \rho_l w_l}{\alpha_g \rho_g + \alpha_l \rho_l}.$$

Two-Fluid Computational Model

A two-step numerical approach is used to solve the system of eleven equations:

At step 1

- eleven two-phase flow equations are solved using the MUSCL-TVDLF hyperbolic solver
- second order MUSCL-TVDLF numerical scheme was elaborated, further developed and applied for the first time to the 3D system of two-fluid flows
- new feature – non-conservative volume fraction equation is solved simultaneously with the balance equations

At step 2

- instantaneous pressure and/(or if needed) velocity relaxation is performed to restore the equilibrium of the two fluids

2D Air-Helium Kelvin-Helmholtz Instability

roll up of initial horizontal air-helium interface

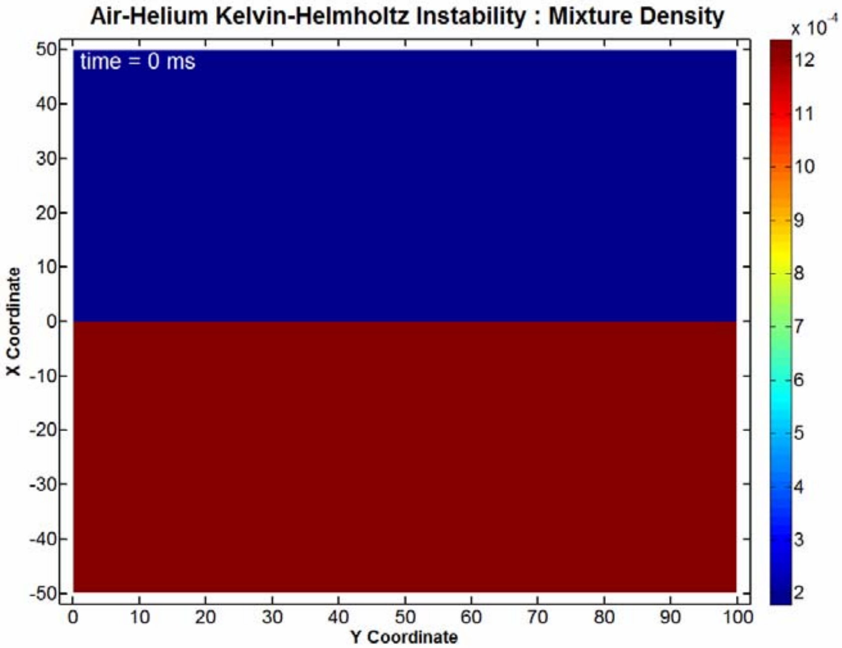

Speed 200 m/s

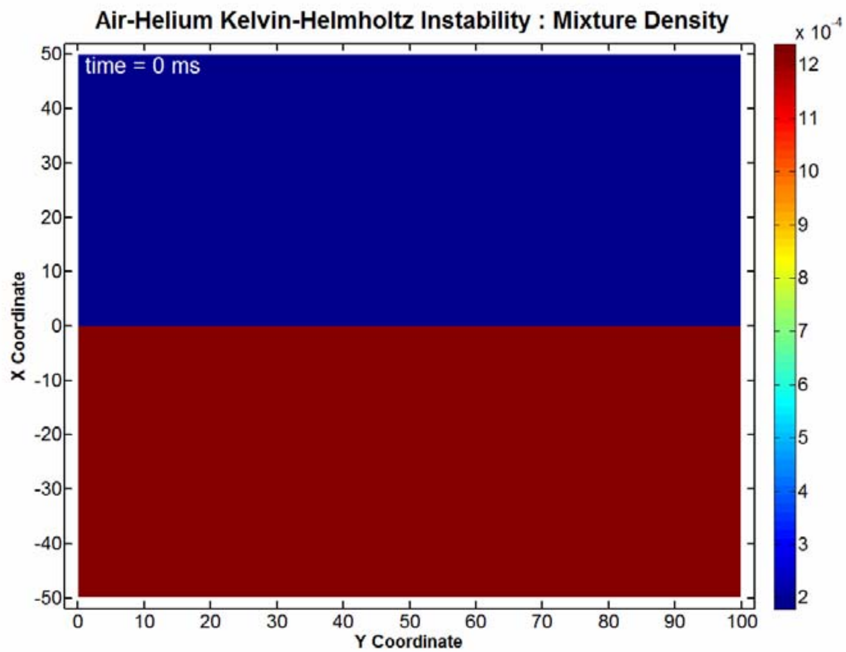

Speed 500 m/s

- broken vortex cores and development of spikes near the interface - variations in air density is necessary condition for K-H
- small vortices and broken droplets dominate in the late stages
- pinch-off of the interface with formation of droplets

PURDUE UNIVERSITY

Plasma-Liquid Tungsten Instability

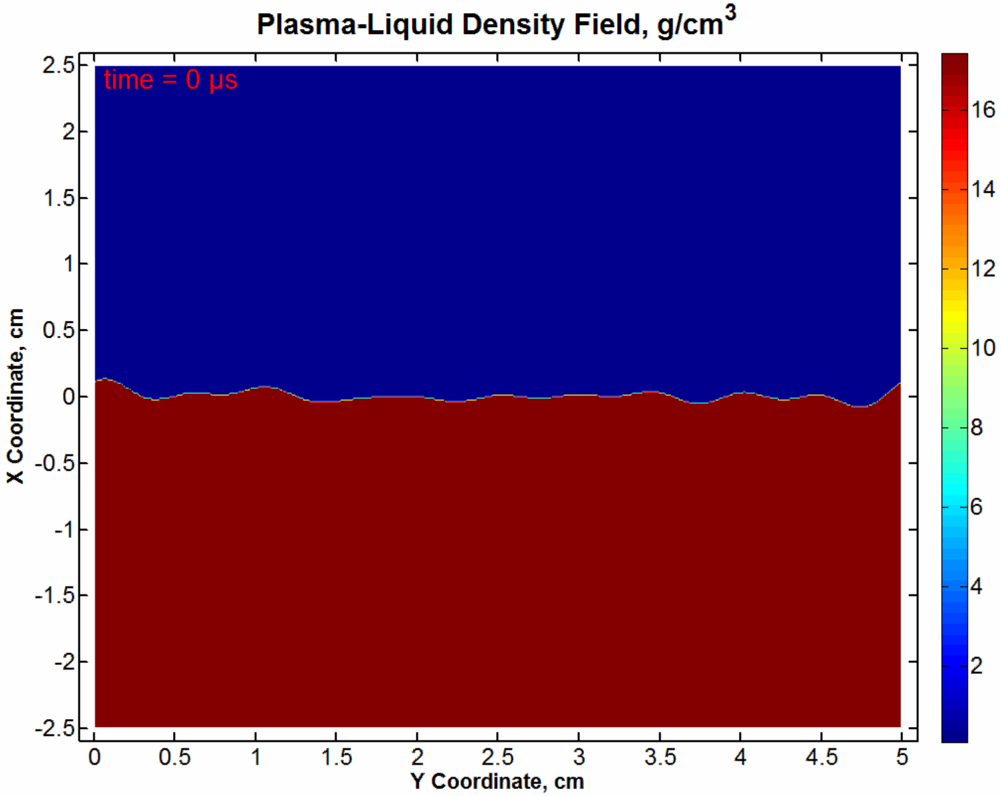

Plasma-liquid interface with random initial perturbation

Plasma density: ~0.01 g/cm^3

Plasma speed: ~10^6 cm/s

- disruption of the interface within the melt depth ~1 cm
- formation of liquid plumes, fingers and droplets drugged by the plasma flow
- topological structure of liquid patters is highly irregular – no periodic array of compact spanwise K-H rollers
- velocity of liquid metal motion is ~2-5 m/s deeply inside the melt layer; the velocity of melt fragments reaches up to ~150 m/s at the surface

PURDUE
UNIVERSITY

Plasma-Liquid Tungsten Instability

1. *Kelvin–Helmholtz instability mechanism: not observed*

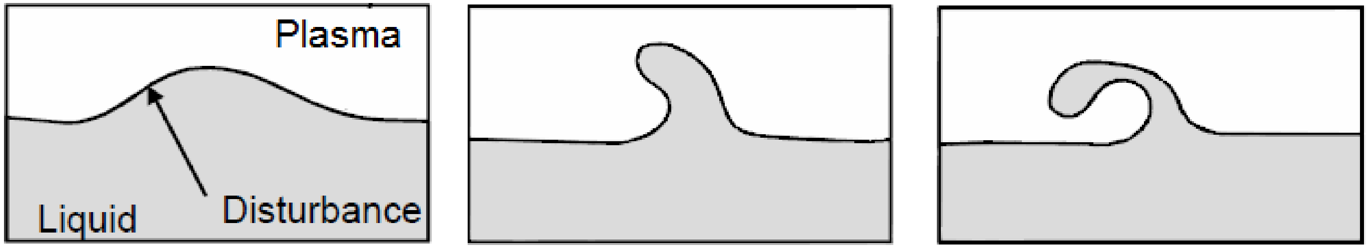

- surface waves amplify forming finger-like projections that break off to form droplets
- depth of the melt affected is of the order of the wavelength of the surface disturbance

2. *Plasma-driven flow instability mechanism: observed*

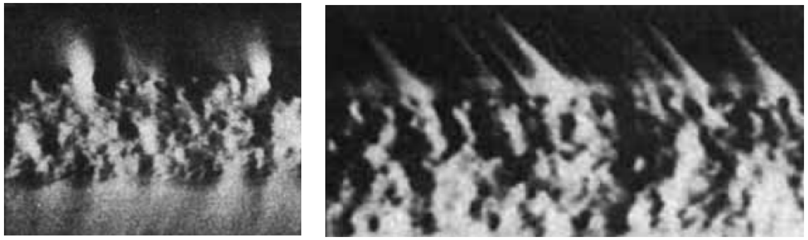

- large droplets can be blown out by shear forces acting on the bulk of the molten metal
- impulse of the plasma flow can cause bulk fragmentation of the melt layer with ejection of large particle fragments

Conclusions

- high-speed (~10^4-10^5 m/s) and dense (>0.01 g/cm^3) plasma flows over the liquid surface can generate the ejection of droplets from a homogeneous melt layer due to bulk shear forces

- introduction of bubbles and density inhomogeneities into a melted layer can significantly change its behavior and cause ejection of droplets for lower plasma densities and speeds

- for typical ELM parameters, these predictions mean no melt splashing and droplet ejection from melt surface due to the K-H instability induced by plasma flow; JxB force could be the main mechanism